



HAL
open science

Efficient degradation of the organic UV filter benzophenone-3 by *Sphingomonas wittichii* strain BP14P isolated from WWTP sludge

Sonja K. Fagervold, Clémence Rohée, Alice M. S. Rodrigues, Didier Stien,
Philippe Lebaron

► To cite this version:

Sonja K. Fagervold, Clémence Rohée, Alice M. S. Rodrigues, Didier Stien, Philippe Lebaron. Efficient degradation of the organic UV filter benzophenone-3 by *Sphingomonas wittichii* strain BP14P isolated from WWTP sludge. *Science of the Total Environment*, 2021, 758, pp.143674. 10.1016/j.scitotenv.2020.143674 . hal-03217024

HAL Id: hal-03217024

<https://hal.science/hal-03217024v1>

Submitted on 4 May 2021

HAL is a multi-disciplinary open access archive for the deposit and dissemination of scientific research documents, whether they are published or not. The documents may come from teaching and research institutions in France or abroad, or from public or private research centers.

L'archive ouverte pluridisciplinaire **HAL**, est destinée au dépôt et à la diffusion de documents scientifiques de niveau recherche, publiés ou non, émanant des établissements d'enseignement et de recherche français ou étrangers, des laboratoires publics ou privés.

1 Efficient degradation of the organic UV filter benzophenone-3 by *Sphingomonas*
2 *wittichii* strain BP14P isolated from WWTP sludge

3

4 S. K. Fagervold^{1*}, C. Rohée², A. M. S. Rodrigues¹, D. Stien¹ and P. Lebaron¹

5

6 ¹ Sorbonne Université, CNRS, Laboratoire de Biodiversité et Biotechnologies
7 Microbiennes, LBBM, Observatoire Océanologique, 66650 Banyuls-sur-mer, France

8 ² Pierre Fabre Dermo-Cosmétique, Centre de Recherche & Développement Pierre
9 Fabre, 31000 Toulouse

10

11 * Corresponding author: Sonja K. Fagervold. fagervold@obs-banyuls.fr.

12 Address: Observatoire Océanologique de Banyuls, Laboratoire de Biodiversité et
13 Biotechnologies Microbiennes, Avenue Pierre Fabre, 66650 Banyuls/mer, France

14

15

16 **Abstract**

17 Benzophenone-3 (BP3) is a widely used organic UV filter present in many
18 environmental compartments. One way BP3 is released into the environment is
19 through effluents from wastewater treatment plants (WWTPs). These plants are
20 possible sources for degradation activity as WWTP sludge can potentially degrade
21 BP3. Our goal was to identify the BP3 degrading microorganism(s) in WWTP sludge
22 and to investigate whether the degradation was co-metabolic. Initial WWTP sludge
23 microcosms spiked with BP3 showed 100% degradation after 20 days. Multiple

24 transfers of these microcosms, while maintaining a strong selective pressure for
25 BP3 degradation capabilities, resulted in the dominance of one bacterial strain. This
26 strain, *Sphingomonas wittichii* BP14P was subsequently isolated and shown to
27 degrade BP3 in a growth dependent manner. Strain BP14P utilized BP3 as the sole
28 energy and carbon source and completely degraded BP3 after 7 days in minimal
29 media. We tested the capability of BP14P to degrade nine other UV filters, but the
30 degradation ability seemed to be restricted to BP3. However, whether this
31 specificity is due to the lack of degradation genes, cellular transport or low
32 bioavailability of the other UV filters remained unclear. The efficient degradation of
33 BP3 by a group of bacteria well known for their potential for xenobiotic degradation
34 is an important step forward for a complete risk assessment of the long-term
35 environmental impact of BP3.

36

37 **Keywords:** Sunscreens, BP3 degradation, growth-dependent, *Sphingomonas*
38 *wittichii*

39

40 **1. Introduction**

41 Benzophenone-3 (BP3) is an organic UV filter commonly used in sunscreen
42 formulations and other cosmetic products. Due to its widespread use, BP3 is now
43 found in many environmental compartments such as freshwater and seawater,
44 benthic sediments and aquatic biota (see Mao et al. (2018) for a recent review).
45 Further, BP3 has been found in bird eggs (Molins-Delgado et al., 2017) and even in
46 human breast tissue (Barr et al., 2018) suggesting that BP3 can biomagnify. Also, it

47 has been demonstrated that BP3 can be absorbed through the skin but the effects of
48 elevated systemic BP3 concentrations in humans are still unclear (Suh et al., 2020).
49 BP3 has been shown to be toxic in several species used for toxicological testing
50 including fish, corals and algae (see recent review and references therein (Lozano et
51 al., 2020)). Thus, the toxicity of BP3 combined with the possibility of
52 bioaccumulation indicates that BP3 might pose an ecological risk (Díaz-Cruz et al.,
53 2019).

54

55 Wastewater treatment plants (WWTPs) are a major source of BP3 to the
56 environment, in addition to recreational water activities and industrial wastewater
57 discharges (Mao et al., 2018). Indeed, BP3 has been found in influents and effluents
58 of WWTPs (Ramos et al., 2016; Mao et al., 2018) in relatively high concentrations.
59 Often, the concentrations of BP3 are lower in the effluents of WWTPs than the
60 influents. This difference can be attributed to sorption to activated sludge and/or
61 biodegradation.

62

63 Biodegradation of BP3 has been shown to occur in different systems. Liu and
64 colleagues observed degradation of BP3 in activated sludge microcosms (Liu et al.,
65 2012) and in microcosms using aquifer materials as an inoculum (Liu et al., 2013).
66 The data from this latter study was used as input in a model to better understand
67 the fate of UV filters, including BP3, in aquifers (Rodríguez-Escales and Sanchez-Vila,
68 2020). Among others, this model took into account sorption processes, both to
69 sediments and biomass, but also assumed that the UV-filters were degraded in a co-

70 metabolic manner with the oxidation of sediment organic matter as the main
71 process.

72

73 The microorganisms responsible for the degradation in the studies described above
74 were not identified (Liu et al., 2012; Liu et al., 2013). So far the only bacterial strain
75 shown to be capable of BP3 degradation is *Methylphilus* sp. strain FP-6, which
76 degraded BP3 co-metabolically when grown with several other carbon substrates
77 (Jin et al., 2019). The white root fungus *Trametes versicolor* can also degrade BP3
78 (Badia-Fabregat et al., 2012; Gago-Ferrero et al., 2012) but it is not known if this
79 degradation was a co-metabolic process since dried and sterilized sludge was used
80 as solid support in these experiments.

81

82 The objective of our study was to investigate the potential degradation of BP3 in
83 microcosms with WWTP sludge, to determine whether the BP3 degradation is
84 indeed co-metabolic and whether any bacterial species exist that can completely
85 mineralize BP3.

86

87

88 **2. Materials and methods.**

89

90 *2.1 Chemicals*

91 The UV filters used for biodegradation studies, 2-hydroxy-4-methoxybenzophenone
92 (BP3) and methylene bis-benzotriazolyl tetramethylbutylphenol (MBBT) were

93 purchased from Sigma-Aldrich (Lyon, France), while 2-ethylhexyl salicylate (ES),
94 homosalate (HS), butyl methoxydibenzoylmethane (BM), octocrylene (OC),
95 diethylamino hydroxybenzoyl hexyl benzoate (DHHB), diethylhexyl butamido
96 triazone (DBT), and ethylhexyl triazone (ET) were kindly provided to us by Pierre
97 Fabre Pharmaceuticals. Analytical standards for the above-mentioned UV filters
98 were purchased from Sigma-Aldrich (Saint-Quentin-Fallavier, France). Analytical-
99 grade dichloromethane (DCM), 1-methyl-2-pyrrolidinone (NMP), methanol, formic
100 acid (98 %) and molecular grade formaldehyde were obtained from Sigma-Aldrich.
101 Pure water was obtained from an Elga Purelab Flex System (Veolia LabWater STI,
102 Antony, France). Glassware was cleaned with DCM and calcinated at 450 °C for 2
103 hours to remove all traces of organic matter.

104

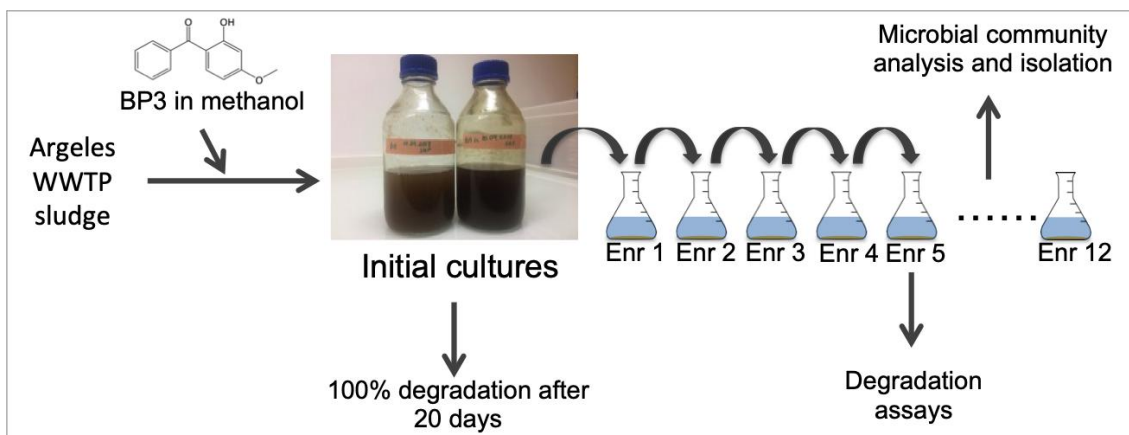
105 *2.2 Sampling of sludge, initial culture and enrichment culture setup*

106 The sludge was sampled from the Argelès-sur-mer (France) wastewater treatment
107 plant (WWTP) on August 24th, 2018, from the bottom of a clarifying tank. The
108 sludge was collected in glass mason jars and stored at 4 °C until utilized for
109 degradation experiments. The sludge contained 2765 (+/- 310) mg/L total
110 suspended solids (TSS) and the initial BP3 concentration was below the detection
111 limit for our analysis (4.6 ng/g, see Fagervold et al. (2019)). For the initial
112 degradation experiments, 100 mL sludge was mixed with 500 mL freshwater
113 mineral media (OECD301) in a 1-L glass bottle (live). BP3 was added in methanol (2
114 mg/mL) to a final concentration of 10 µg/ml. A sterile control (SC) was prepared by
115 autoclaving twice (48 hours apart) a 1-L bottle containing sludge and media at 120

116 °C for 20 minutes, followed by the addition of sodium azide (1 %) and then BP3. The
117 two bottles (one live and one SC) were incubated at 25 °C in the dark and were
118 systematically shaken and opened inside a fume hood twice per week to allow
119 aeration.

120

121 An enrichment culture was initiated with inoculum from the initial flask that
122 showed degradation. The final theoretical BP3 concentration was about 10 µg/mL
123 for Enrichment 1 (the first transfer), but this concentration was increased to a
124 theoretical concentration of 100 µg/mL for Enrichment 2 and subsequent
125 enrichments. To obtain a concentration of 100 µg/mL, 2 mL of a solution of BP3 in
126 acetone (2.5 mg/mL) was added to 100-mL Erlenmeyer flasks containing 2 g of inert
127 sand. The acetone was left to evaporate overnight. Mineral media (50 mL, as above)
128 was added and the flasks were autoclaved. Each month, the cultures were
129 transferred (1% vol/vol) into new flasks with sand and BP3 (see Figure 1 for
130 diagram of the experimental setup). The cultures were incubated at 25 °C in the
131 dark on a platform shaker at 100 rpm.



132

133 **Fig. 1.** Schematic of the experimental design.

134
135
136
137
138

Table 1
Selected chemical properties and structure of the UV filters used in this study (ordered by increasing molecular weight). Note the abbreviations that are used throughout.

Compound name (abbreviation) [CAS number]	MW	Biodegradation rate ^a	Freshwater solubility at 25 °C (mg/L) ^b	LogP ^c	Chemical structure
Benzophenone-3 (BP3) [131-57-7]	228.2	100 %	130	3.514	
2-Ethylhexyl salicylate (ES) [118-60-5]	250.3	15 % 28 % with R2B or BP3	137	5.335	
Homosalate (HS) [118-56-9]	262.3	18 % with R2B or BP3	< LOD (LOD = 0.85)	5.431	
Butyl methoxydibenzoylmethane (BM) [70356-09-1]	310.4	n.d.	19	5.391	
Octocrylene (OC) [6197-30-4]	361.5	n.d.	9.1	7.083	
Diethylamino hydroxybenzoyl hexyl benzoate (DHHB) [302776-68-7]	397.5	n.d.	Not measured	7.078	
bis-Ethylhexyloxyphenol methoxyphenyl triazine (BEMT) [187393-00-6]	627.8	n.d.	0.3	10.627	
Methylene bis-benzotriazolyl tetramethylbutylphenol (MBBT) [103597-45-1]	658.9	n.d.	< LOD (LOD = 0.04)	15.451	
Diethylhexyl butamido triazone (DBT) [154702-15-5]	766.0	n.d.	0.2	12.004	
Ethylhexyl triazone (ET) [88122-99-0]	823.1	n.d.	Not measured	14.589	

^a Degradation rate at day 14, when no degradation is seen in SC, and when p < 0.05 compared to SC with a Student t-test. n.d. stands for no degradation.
^b Experimental data. See protocol in Fagervold et al. (2019). LOD: Limit of detection.
^c According to Reaxys database (<https://www.reaxys.com/>, accessed on June 9, 2020)

139
140

141 *2.3 Biodegradation assays*

142 Biodegradation assays were conducted using 15-mL glass tubes with Teflon lined
143 caps (Pyrex, Analytic lab, France). The tubes were set up as for the enrichment
144 cultures, but with 0.2 g sand, 3 mL media, and care was taken so that for each batch
145 of degradation assays, the exact same amount of BP3 (around 100 µg/mL) was
146 added to the tubes. Three tubes were sacrificed for each time-point. The tubes were
147 incubated at 25 °C after inoculation. For the enrichment cultures, the inoculum for
148 the assay was 150 µL of supernatant after rigorous mixing of the enrichment
149 culture. Inoculum preparation for the biodegradation assay of strain BP14P was
150 done as follows: The strain was grown in 100 % R2B broth (Thermo Fisher
151 Scientific, Illkirch-Graffenstaden, France) for about 40 h until the culture had
152 reached an optical density at 600nm of approximately 1.0. The cell suspension was
153 centrifuged at 4200 g for 10 min and subsequently washed 2 times with minimal
154 media before a final resuspension in minimal media (4% v/v). The cultures were
155 incubated at 25 °C in the dark on a rotary shaker at 100 rpm.

156

157 *2.4 BP3 extraction*

158 Two different protocols were used for the extraction of BP3, one for the initial
159 biodegradation experiments and another for the biodegradation assays for
160 enrichment cultures and isolated strains.

161

162 For the initial cultures containing WWTP sludge, 5 mL slurry was taken in duplicate
163 from each flask for each timepoint, both live and SC. The slurry was centrifuged (950

164 x g for 20 min) to separate the aqueous and solid phases. The aqueous and solid
165 phases were then extracted and analyzed separately. The supernatant (aqueous
166 phase) was transferred to a new tube and subjected to liquid/liquid extraction with
167 acidified (0.1 % formic acid) DCM. This was achieved by adding 5 mL acidified DCM
168 to the aqueous sample, mixing by vortexing and shaking overnight at 25 °C in the
169 dark. The DCM fraction was decanted off and dehydrated with Na₂SO₄. The DCM was
170 then evaporated using the HT-4X system (Genevac, Biopharma Technologies,
171 Diemoz, France) and the residue was dissolved in 1 mL of NMP/water (8:2, v/v)
172 before analysis.

173

174 The solid phase was extracted as described by Fagervold and coworkers (Fagervold
175 et al., 2019) with modifications. Briefly, the pellet was frozen at -80 °C, lyophilized
176 and extracted twice with 2 ml acidified (0.1% formic acid) DCM/methanol mix (1:1,
177 vol/vol) and sonicated for 10 min. The supernatants were combined, evaporated
178 and re-dissolved in NMP/water (8:2, v/v) before HPLC analysis.

179

180 For the biodegradation assays, the whole tube containing sand and liquid media was
181 sacrificed for extraction at each timepoint. DCM (3 mL) containing an exact known
182 amount of MBBT (internal standard) was added to each tube. The tubes were mixed
183 by vortexing twice for 10 seconds, 1 h apart and shaken overnight at 100 rpm at 25
184 °C in the dark. After a brief sonication, 1 mL of the DCM phase was transferred to a
185 HPLC vial and diluted 20X in DCM before HPLC analysis.

186

187 *2.5 HPLC analysis*

188 The UV filters were analyzed using an Ultimate 3000™ HPLC system, equipped with
189 a DAD detector (Thermo Fisher Scientific) and a Phenomenex Kinetex Biphenyl 2.6
190 µm, 150 × 4.6 mm column as previously described (Fagervold et al., 2019) with
191 some minor modifications. The injection volume was 5 µl and the samples were
192 diluted in 100% DCM. We expanded the analysis described in Fagervold et al.
193 (2019) to include all targeted UV-filters. The calibration curves and retention times
194 of all the different UV filters (Table 1) were determined as described by Fagervold
195 and coworkers (Fagervold et al., 2019). The recovery rate was above 85 % for the
196 extraction of BP3 in the initial sludge microcosms. The recovery rate for the
197 degradation assays were variable for the different UV filters, ranging from 63 % for
198 ES to 93 % for OC. However, the extraction efficiency was repeatable for each UV
199 filter over time, which is the most important factor for the detection of degradation
200 activity.

201

202 For determination of possible BP3 degradation products, we also performed a
203 UHPLC-MS/MS analyses as described by Stien and coworkers (Stien et al., 2019).
204 The data were acquired using the Trace Finder™ 3.1 software and were processed
205 with FreeStyle™ and Compound Discoverer™ (all from Thermo Fisher Scientific).

206

207 *2.6 Microbial community analysis of enrichment cultures*

208 DNA was extracted using a Maxwell® 16 LEV Blood DNA Kit (Promega,
209 Charbonnières-les-Bains, France) with the Maxwell® 16 MDx Instrument (AS3000;

210 Promega) following the manufacturer's instructions and with an initial lysing step.
211 Briefly, 2 mL of supernatant was transferred to a microcentrifuge tube and
212 centrifuged at 14 500 x g for 10 minutes. The pellet was resuspended in 300 µL
213 MilliQ water and 300 µL of the lysing buffer from the Maxwell® 16 LEV Blood DNA
214 Kit was added to "lysing matrix B beads" (MP Biochemicals, Illkirch, France) and
215 homogenized for 20 s at 6 m/s on a FastPrep-24™ 5G Instrument (MP biochemicals).
216 After extraction, the DNA was stored at -80 °C until further analysis.
217 The composition and diversity of the bacterial communities in enrichment cultures
218 were determined by Automated Ribosomal Intergenic Spacer Analysis (ARISA) and
219 by Illumina sequencing (RTL genomics, Texas, USA). The ARISA was performed as
220 described by Fisher et al. (Fisher MM and Triplett EW, 1999) with minor
221 modifications. Briefly, for the PCR we utilized the intergenic spacer primers 1406F
222 and 23SRY (Fisher MM and Triplett EW, 1999) and the KAPA2G Fast HotStart
223 ReadyMix (Roche, Analytic Lab, St Mathieu de Treviers, France) with the following
224 PCR cycling parameters: 94 °C for 3 minutes, 30 cycles of 94 °C for 15 s, 55 °C for 15
225 s and 72 °C for 30 s, then a final elongation of 72 °C for 1 min. The products were
226 purified, denatured and injected into a 16 capillary Applied Biosystems Sequencer
227 3130XL (Thermo Fisher Scientific) together with the internal standard
228 MapMarker® X-Rhodamine Labeled 50-1000 bp (Bioventures Inc., Tennessee, USA)
229 for the determination of peak lengths. For the analysis, individual fragment lengths
230 (within a 0.1 bp "error range") were considered as separate Operational Taxonomic
231 Units (OTUs) and the relative abundance of each OTU was calculated by dividing the
232 area of the peak by the total area of the chromatogram after 200 bp. Furthermore,

233 we only took into account peaks contributing to more than 1 % of the relative peak
234 area. Concerning the Illumina sequencing analysis, the DNA was sent to RTL
235 genomics where paired end, 2×300 bp MiSeq Sequencing was performed using
236 standard conditions of the sequencing provider. We opted for dual indexing and
237 used the bacterial primers 341F (CCTACGGGNGGCWGCAG) and 806R
238 (GACTACHVGGGTATCTAATCC) (Herlemann et al., 2011). The sequences were
239 processed using Qiime2 (Bolyen et al., 2019). Briefly, the sequences were quality
240 filtered, stitched, denoised and clustered using dada2. Representative sequences
241 were classified using the Naive Bayes classifier and the Silva 132 database as a
242 reference. Our two samples (Enr 11 and Enr 12) yielded about 41000 and 47000
243 sequences, of which 39000 and 44000, respectively, belonged to a single OTU. There
244 were a total of 37 OTUs in the two samples, but most were present at very low
245 relative abundances.

246

247 *2.7 Strain isolation and sequencing*

248 The supernatant of an actively degrading enrichment culture transferred 7 times
249 (Enrichment 7, or Enr 7) was diluted 100 fold and spread on R2B agar and
250 incubated for 3 days at 25 °C in the dark. Several colony morphologies were
251 observed and each morphotype was re-streaked on R2B agar to ensure purity.
252 These strains were tested for BP3 degradation activity and one positive strain,
253 BP14P, was further characterized. DNA was extracted as described above and
254 sequenced on the same sequencer used for ARISA. Here, we used universal bacterial
255 primers 27F and 1492R in the first PCR and then the internal primers 907R, 804F

256 and S8 for the sequencing reactions realized by the dideoxy reaction Sanger
257 sequencing using the BigDye™ Terminator v3.1 Cycle Sequencing Kit (Thermo
258 Fischer) and the manufacturer's protocol.

259

260 *2.8 Flow Cytometry*

261 Strain BP14P cells were counted throughout the degradation assay. The glass tubes
262 were vortexed and 1 mL of cell suspension was transferred to a microcentrifuge
263 tube before adding glutaraldehyde (1% v/v final concentration). The tubes were
264 incubated at 4 °C in the dark for 15 minutes before flash freezing with liquid N₂. The
265 samples were kept at -80 °C until analysis. Samples were defrosted at room
266 temperature and incubated with the nucleic acid stain SYBRGreen I (Molecular
267 Probes) for 15 min at room temperature in the dark before enumeration (Marie et
268 al., 1997) using a FACSCanto flow cytometer (BD-Biosciences) equipped with optics
269 fiber emitted light (407, 488 and 633 nm). Fluorescent 1.002 µm beads
270 (Polysciences Inc., Europe) were added to each sample as an internal standard to
271 normalize cell properties and to compare cell populations. Accurate analyzed
272 volumes and subsequent estimations of cell concentrations were calculated using
273 Becton-Dickinson Trucount™ beads. Total bacterial cells (TBA) were enumerated
274 according to the variations of light scatter properties (relative cell size) and green
275 fluorescence related to nucleic acid content.

276

277

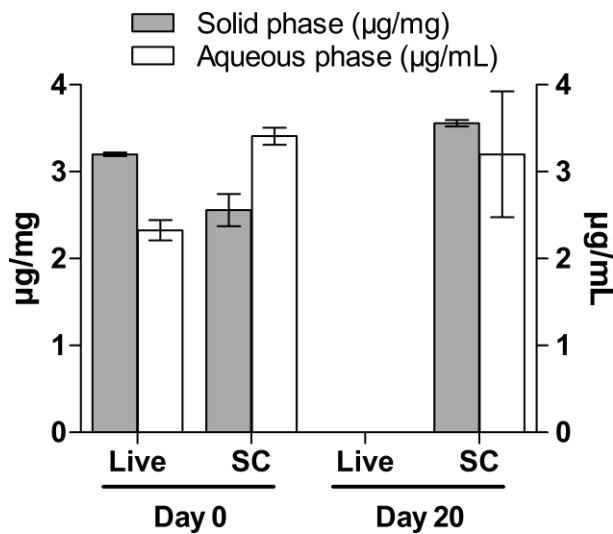
278 **3. Results and discussion**

279

280 3.1 Degradation of BP3 in initial sludge microcosms and enrichment cultures

281 To detect BP3 degradation, the concentration of BP3 in the amended flask
282 containing active sludge was compared with the amended flask containing sterilized
283 sludge. The theoretical added total BP3 concentration was 10 $\mu\text{g}/\text{mL}$ slurry and the
284 slurry contained approximately 2 mg/mL dry matter. We analyzed the aqueous and
285 the solid phase separately and it was clear that some BP3 partitioned onto the solid
286 phase in the slurry (Figure 2). This fraction was bioavailable since we could not
287 detect any BP3 in either the solid or the aqueous phase after 20 days of incubation.
288 The concentration in the SC remained approximately the same after 20 days,
289 showing that this is not an artifact due to abiotic sorption processes. Thus, we
290 observed a complete degradation of BP3 in live cultures compared to the SC after 20
291 days.

292



293

294 **Fig. 2.** BP3 concentrations in initial microcosms with WWTP sludge. BP3

295 concentrations in the aqueous phase ($\mu\text{g}/\text{mL}$, white bars) and in the solid phase (μ

296 g/mg, grey bars) at day 0 and after 20 days of incubation. Live, active degrading
297 slurries and SC, sterile control.

298

299 The live culture actively degrading BP3 was transferred into an Erlenmeyer flask
300 containing 10 µg/mL BP3 (Enrichment 1, Enr 1). After 30 days, the Enr 1 culture
301 was transferred into a flask containing a higher BP3 concentration (100 µg/mL)
302 (see figure 1), Enr 2. We added sand to the flasks with the hypothesis that it may
303 provide a solid support for the microorganisms. The cultures were transferred
304 every 30 days to further enrich BP3 degrading microorganisms. To maintain a
305 selective pressure on the microbial community, the only available carbon source for
306 the microorganisms was BP3. We could clearly see growth in the Erlenmeyer flask
307 based on the turbidity of the medium.

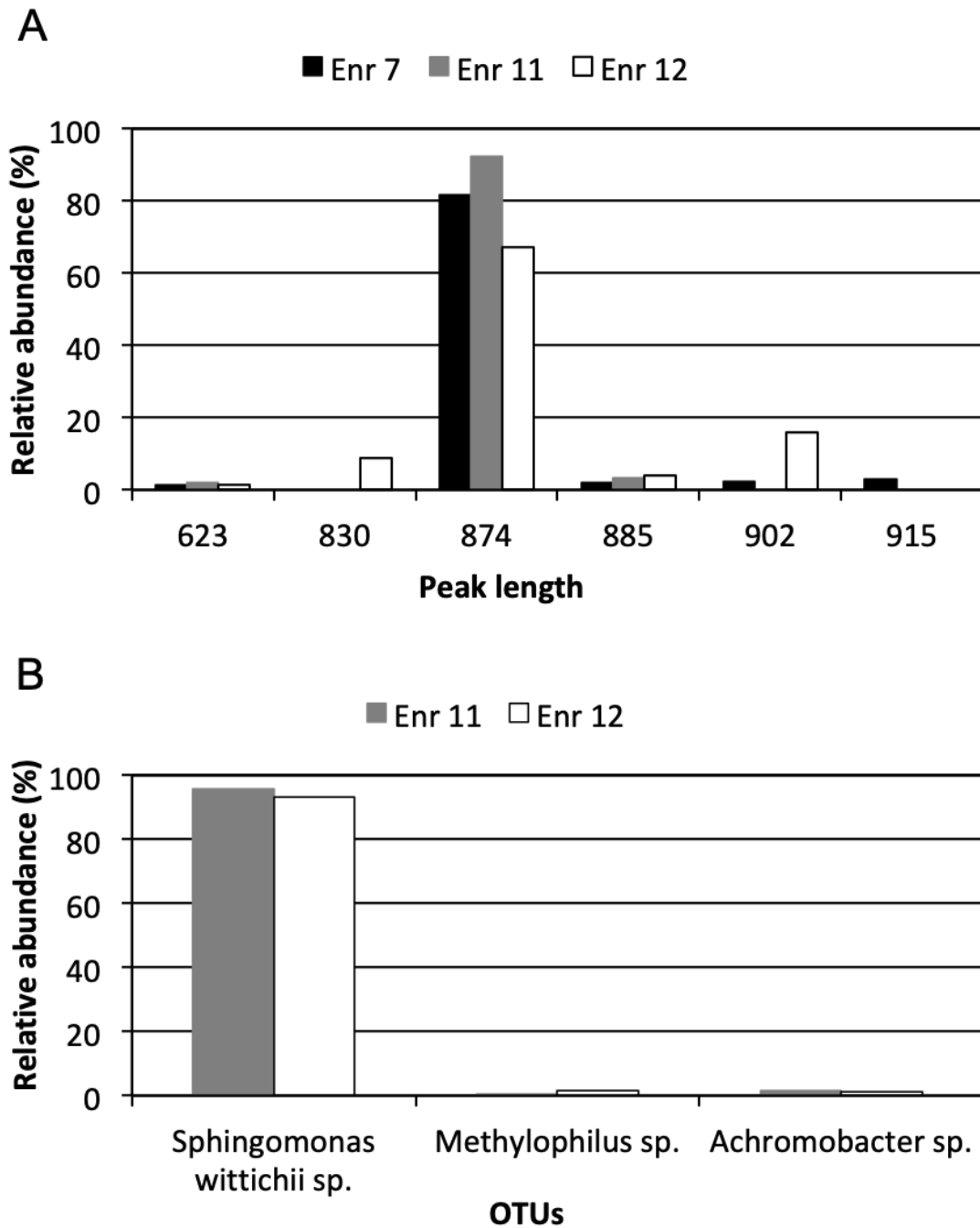
308

309 After 5 consecutive transfers, we verified the degradation activity of the Enr 5
310 enrichment culture by performing biodegradation assays in separate tubes. After 7
311 days of incubation, we could only detect trace amounts BP3 in the live
312 biodegradation assays, while the SC showed no decrease compared to day-0
313 samples. This was also observed in another biodegradation assay from Enr 9 (after
314 9 transfers) after 5 days. Thus, it was clear that these enriched cultures degrade BP3
315 in a relatively fast manner.

316

317 *3.2 Microbial communities in enrichment cultures*

318



319

320 **Fig. 3.** Analysis of the microbial community diversity in BP3 degrading enrichment
 321 cultures. (A) ARISA analysis of enrichment cultures “Enr 7” (black bars), “Enr 11”
 322 (grey bars) and “Enr 12” (white bars) where each peak is one “OTU” and the relative
 323 abundance is based upon area of each peak. (B) Relative abundance of different

324 OTUs based upon Illumina sequencing in “Enr 11” (grey bars) and “Enr 12” (white
325 bars).

326

327 In order to estimate the diversity and stability of the enrichment cultures degrading
328 BP3, we performed ARISA of several enrichments and confirmed these results with
329 Illumina sequencing. We extracted DNA of cultures at day-4 after transfer and this
330 was done for different transfers (Enr 7, 11 and 12). Briefly, ARISA is based upon the
331 concept that different bacteria have different sized intergenic spacers between the
332 16S rRNA gene and the 23S rRNA gene on their chromosome. An ARISA profile will
333 give an approximation of the microbial diversity of a sample, with one peak
334 representing one “OTU”. From the ARISA we could see 5 different main peaks
335 (Figure 3A) and it was clear that the enrichment cultures were dominated by one
336 specific bacterium corresponding to a peak length of 874 bp. This was confirmed
337 with the results from the Illumina sequencing, where we detected only 3 major
338 OTUs, with a clear dominance of an OTU identified as *Sphingomonas wittichii* with a
339 relative abundance of about 95 % in both Enr 11 and 12 (Figure 3B). We
340 hypothesized that this strain was responsible for the degradation of BP3 in these
341 enrichment cultures.

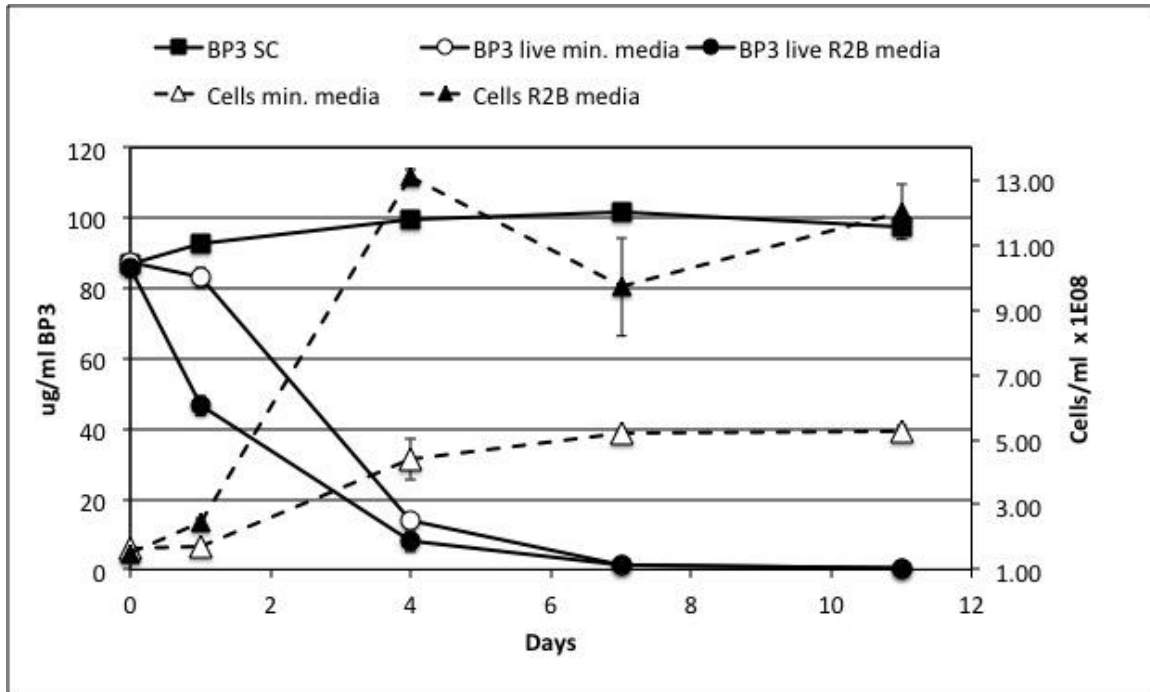
342

343 *3.3 Isolation and identification of the BP3 mineralizing strain BP14P*

344 The most predominant strain in the enrichment cultures, BP14P, was isolated and
345 its degradation capability tested in minimal media (OECD301) and in minimal media

346 amended with 10 % R2B media. This was done to investigate whether strain BP14P
347 would degrade BP3 when other carbon sources were present.

348



349

350

351 **Fig. 4.** Degradation of BP3 by *Sphingomonas wittichii* sp. strain BP14P coupled to
352 growth. BP3 concentrations in sterile controls (black), BP3 concentrations in live
353 cultures with minimal media (open circles), BP3 concentrations in live cultures with
354 minimal media and 10 % R2B media (black circles), cells per ml in cultures with
355 minimal media (open triangles) and cells per ml in cultures with minimal media and
356 10% R2B media (black triangles).

357

358

359 Strain BP14P degraded BP3 relatively fast as we could detect an almost 50%
360 degradation after one day in cultures amended with R2B media, and 90%
361 degradation after 4 days in both cultures with R2B but also in cultures with minimal
362 media (Figure 4). This degradation was clearly linked to growth since the
363 concentration of cells increased with time in cultures where the only carbon source
364 was BP3. We hypothesize that this strain completely mineralized BP3 and used BP3
365 as both carbon and energy source. To the best of our knowledge, this is the first
366 report showing a growth dependent degradation of BP3 in a pure strain.

367

368 A BLAST comparison of the 16S rRNA gene sequence of strain BP14P (1150 bp)
369 showed that it was 100 % identical to *Sphingomonas wittichii* DC-6, isolated from
370 activated sludge (KC410868) and only one base pair different (1149/1150) to the
371 widely studied strain *S. wittichii* RW1 (NR_074268.1). DC-6 can mineralize the
372 herbicides alachlor, acetochlor, and butachlor (Chen et al., 2013) through *N*-
373 dealkylation activity by a Rieske non-heme iron oxygenase system (Chen et al.,
374 2014). *S. wittichii* RW1 was first isolated from an urban river sample (Wittich et al.,
375 1992) and is able to degrade a plethora of aromatic compounds, like chlorinated
376 dibenzo-*p*-dioxins (DDs) and dibenzofurans (DFs) and to grow on DD and DF as sole
377 carbon and energy sources (Wittich et al., 1992). The first step in the degradation of
378 DD and DF is carried out by a dioxygenase and interestingly many of the genes
379 responsible for degradation of aromatic compounds are present on megaplasmids in
380 both strains *Sphingomonas wittichii* RW1 and DC-6 (Armengaud et al., 1998; Cheng

381 et al., 2019; Miller et al., 2010). Indeed, this feature seems to be common in
382 *Sphingomonas* that degrade xenobiotics (Basta et al., 2004).

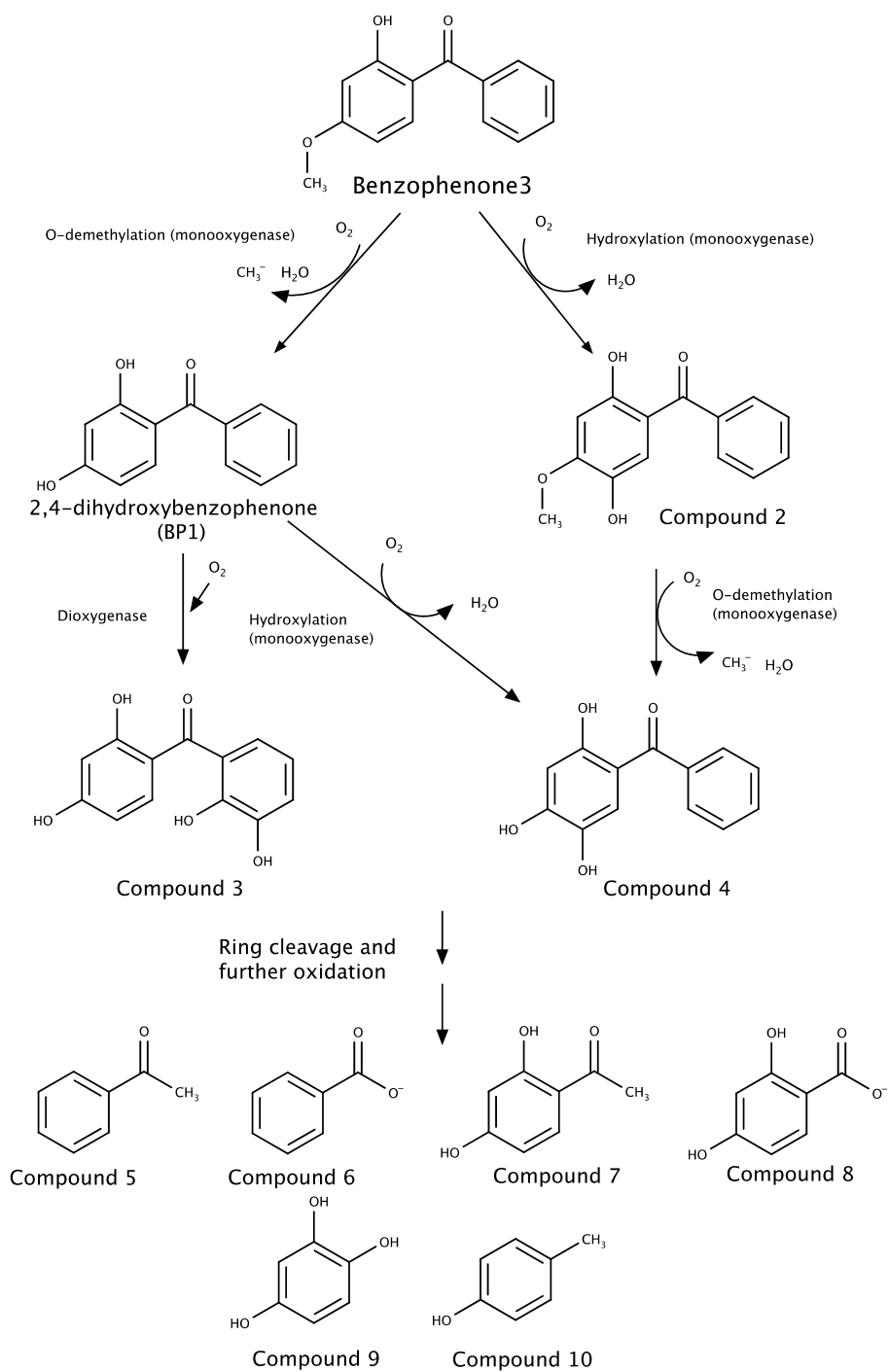
383

384 3.4 Putative degradation pathway of BP3

385 During the HPLC-UV analysis, we could clearly detect an UV absorbing peak at an
386 earlier retention time than BP3 in some samples. To identify this peak and other
387 putative degradation products or intermediates, we analyzed several samples using
388 LC-MS/MS and molecular networks (MN) constructed by means of the Global
389 Natural Products Social Molecular Networking (GNPS) platform (Wang et al., 2016)
390 (<https://gnps.ucsd.edu/>). GNPS is a MS/MS data community sharing and curation
391 platform. Its MN tool organizes all MS/MS spectra recorded in complex mixtures of
392 compounds by families of analogous compounds, each grouped in one MN. This
393 enables the user to highlight possible degradation products in samples without any
394 presupposition of the chemical structure. In the present MN analysis, the number of
395 similar fragments was set to 2, and the minimum cosine for linking two parent ions
396 was set to 0.7. With these parameters, only one compound clustered with BP3, with
397 a parent mass at m/z 215.070 ($[M+H]^+$). This compound was identified as BP1, a
398 BP3 demethylation product (Figure 5). BP1 was detected in high concentrations in
399 day 1 samples of the degradation assay with *S. wittichii* BP14P when R2B was
400 added. At this timepoint, BP3 was already about 50% degraded. This peak was
401 detected only at trace levels in the following timepoints, meaning that BP1 was
402 rapidly degraded. This initial demethylation reaction has been previously reported
403 to be a probable degradation step in activated sludge microcosms (Liu et al., 2012)

404 and as one probable pathway for BP3 degradation by *Methylophilus* sp. strain FP-6
405 (Jin et al., 2019).

406



407

408 **Fig. 5.** Putative degradation pathway of BP3.

409

410 We investigated other possible degradation pathways by submitting the BP3
411 structure to an online pathway prediction tool (Gao et al., 2010) and then searching
412 for particular exact masses of the predicted products (m/z of corresponding $[M+H]^+$
413 ions) in all the LC-MS profiles of our samples. Based upon the prediction, another
414 possible first step is a hydroxylation of the benzene ring (Compound **2** in Figure 5).
415 An ion corresponding to this compound was detected in some of our samples, as
416 was compound **4**. However, we did not detect compound **3** in any of our samples.
417 Based upon these results we hypothesize that the main degradation pathway
418 involves an initial demethylation of BP3 to BP1, followed by a hydroxylation to give
419 **4**. However, an initial hydroxylation of BP3 yielding compound **2** and a following
420 demethylation to result in compound **4** might be a minor pathway.

421

422 Jin and colleagues identified other compounds in *Methylophilus* sp. strain FP-6
423 cultures degrading BP3 (Jin et al., 2019). The presence of these compounds, not
424 depicted in Figure 5, suggested a degradation pathway involving hydroxylation of
425 BP3 and ring cleavage, but no demethylation. We did not find any evidence for this
426 pathway in *S. wittichii* BP14P. This might be due to the different nature (co-
427 metabolism versus growth linked) of the degradation process of the two different
428 strains in question.

429

430 Compounds **5-9** are examples of possible products after cleavage based upon the
431 prediction system. However, these low molecular weight compounds could not be
432 detected by our LC system that analyzed molecules between 133 Da and 2000 Da.

433 Compound **10** was detected by Liu et al. (2012), but was not predicted by the
434 prediction tool.

435

436 *3.5 UV filter degradation capabilities of strain BP14P are limited*

437 We tested the capability of *S. wittichii* BP14P to degrade other UV filters, listed in
438 Table 1. Indeed, Miller et al. (2010) suggest that one of the reasons why *S. wittichii*
439 RW1 is so successful at degrading substrates with low water solubility might be
440 because of the abundance of TonB-dependent receptors, which can act as
441 transporters of aromatic compounds. Further, because the expression of some
442 dioxygenases (like dioxygenases dxnA1A2) have shown to be substrate dependent
443 (Armengaud et al., 1998), we also added BP3 to parallel assays to investigate
444 whether the putative expression of genes involved in degradation of BP3 can
445 stimulate the degradation of other aromatic compounds. Accordingly, we tested the
446 UV filters listed in Table 1 alone in biodegradation assays, as well as with extra
447 carbon (10% R2B) and with BP3.

448

449 We incubated *S. wittichii* sp. BP14P with the 9 different UV filters for 14 days. BP3
450 was over 95% degraded in all the assays where it was added. However, we detected
451 very little degradation of the other UV filters (Table 1). The only other UV filter that
452 was partially degraded with no other carbon sources present was ES (15 % after 14
453 days). *S. wittichii* BP14P degraded ES slightly more when BP3 and other carbon
454 sources were present, namely 28 % after 14 days. Finally, HS was 18 % degraded
455 after 14 days when BP3 and other carbon sources were present.

456

457 To summarize, *S. wittichii* BP14P did not degrade other UV filters to a great extent.
458 This specificity could be due to limited bioavailability of the other UV filters, a
459 limitation of putative transporters, or potentially, a limitation in the genes involved
460 in degradation.

461

462 *3.6 What drives the specificity of BP3 degradation by strain BP14P?*

463 Other researchers have observed that BP3 can be biodegraded. Liu et al. (2012)
464 found that BP3 was completely degraded after 42 days of incubation in both aerobic
465 and anaerobic microcosms also using inoculum from a WWTP. This suggests that
466 several groups of bacteria could be possible degraders, but this was not investigated
467 by Liu and colleagues. *Methylophilus* sp. strain FP-6 was shown to co-metabolically
468 degrade BP3, degrading 15 % of BP3 after 8 days when no other carbon source was
469 provided but degrading BP3 to a higher extent when other carbon sources were
470 present (Jin et al., 2019). Based on the data provided, we believe that *Methylophilus*
471 sp. strain FP-6 degraded BP3 co-metabolically. Strikingly, strain BP14P was very
472 specifically enriched in the cultures through many transfers, suggesting there were
473 no other bacteria present in the sludge that could degrade BP3 in a growth
474 dependent manner or in an equally efficient manner as strain BP14P.

475

476 Even though the 16S rRNA gene of strain BP14P was 99.99% and 100% identical to
477 *S. wittichii* RW1 and DC-6, respectively, the functional similarity between these
478 strains remains to be investigated through a more polyphasic approach, including

479 genome sequencing. Interestingly, *S. wittichii* RW1 has a very specific dioxygenase
480 activity that enables it to degrade DD and DF (Armengaud et al., 1998) and thus we
481 hypothesize that *S. wittichii* BP14P degrades BP3 through the activity of at least one
482 specific mono- or dioxygenase responsible for the initial demethylation (see figure
483 4) or another limiting step in the degradation pathway. We base this hypothesis on
484 the fact that the mono- or dioxygenase activity needed for BP3 degradation did not
485 seem to be widely distributed as no other bacteria were enriched in these cultures.
486 However, whether it uses a homologue of the *S. wittichii* RW1 enzyme, remains to be
487 investigated.

488

489 *S. wittichii* strains seem to be especially suited to degrade xenobiotics. For example
490 *S. wittichii* RW1 has extreme redundancy in its use of aromatic compound
491 metabolism (Coronado et al., 2012). This group of microorganisms generally
492 contains megaplasmids containing degradation genes and horizontal gene transfer
493 seems to be very common. Importantly, it is well known that *S. wittichii* RW1 can
494 survive and retain its degradation capability in soil when amended for
495 bioremediation purposes (Megharaj et al., 1997). All this makes it particularly
496 fascinating to enlarge the degradation repertoire of this group to include UV filters
497 and BP3.

498

499 **4. Conclusions and perspectives**

500 The extensive use of BP3 has resulted in ubiquitous BP3 contamination in various
501 environments, including in WWTPs and in many aquatic ecosystems (Fagervold et

502 al, 2019). For a complete environmental risk assessment of BP3, it is important to
503 understand its fate and all the processes the molecule is subjected to. Degradation,
504 though either co-metabolism or mineralization is an important factor in this
505 assessment. We show here that BP3 can be completely degraded in a few days in
506 WWTPs by *S. wittichii* BP14P. Since BP3 can be utilized by a bacterium as an energy
507 source it then ensues that BP3 has the potential to be degraded in other
508 environmental compartments than WWTP sludge. As a consequence, the long-term
509 accumulation of BP3 in the environment could be less likely than previously
510 assumed. However, once released into marine ecosystems, it is as yet unknown
511 whether BP3 can be degraded. This question should be the subject of future studies,
512 as well as performing similar degradation testing on other sunscreen UV filters, with
513 a priority on the most toxic UV filters including octinoxate, octocrylene and
514 homosalate

515

516 **Acknowledgements:**

517 We would like to thank Cécile Villette for performing the sequencing of strain BP14P
518 and Maeva Duboeuf for help with chemical extractions. This work was carried out in
519 conjunction with the European Marine Biological Resource Centre (EMBRC-ERIC-
520 Banyuls-sur-Mer Oceanographic Observatory, OOB). We are grateful to the
521 BIO2MAR platform for providing access to instrumentation and especially to Nyree
522 West for technical help concerning the ARISA procedure and for reading through the
523 manuscript. We would like to thank Christophe Salmeron of the BioPIC Imaging and
524 Cytometry platform (OOB) for performing the flow cytometry and the technical

525 support of EMBRC-France, whose French state funds are managed by the ANR
526 within the Investments of the Future program under reference ANR-10-INBS-02. We
527 would also like to thank the local council (Communauté de Communes Albères-Côte
528 Vermeille-Illibéris) who provided access to the WWTP site for sampling. This work
529 was financially supported by the Pierre Fabre Dermo-Cosmetic Laboratories in
530 France.

531

532 **Figure captions**

533 Figure 1. Schematic of the experimental design.

534

535 Figure 2. BP3 concentrations in initial microcosms with WWTP sludge. BP3
536 concentrations in the aqueous phase ($\mu\text{g}/\text{mL}$, white bars) and in the solid phase ($\mu\text{g}/\text{mg}$, grey bars) at day 0 and after 20 days of incubation. Live, active degrading
537 slurries and SC, sterile control.

539

540 Figure 3. Analysis of the microbial community diversity in BP3 degrading
541 enrichment cultures. (A) ARISA analysis of enrichment cultures Enr 7 (black bars),
542 Enr 11 (grey bars) and Enr 12 (white bars) where each peak is one OTU and the
543 relative abundance is based upon area of each peak. (B) Relative abundance of
544 different OTUs based upon Illumina sequencing in Enr 11 (grey bars) and Enr 12
545 (white bars).

546

547 Figure 4. Degradation of BP3 by *Sphingomonas wittichiii* sp. strain BP14P (left axis)
548 and growth followed by flow cytometry (right axis). BP3 concentrations in sterile
549 controls (SC, black square), BP3 concentrations in live cultures with minimal media
550 (open circles), BP3 concentrations in live cultures with minimal media
551 supplemented with 10 % R2B media (black circles), cell concentrations of cultures
552 with minimal media (open triangles) or minimal media supplemented with 10%
553 R2B media (black triangles).

554

555

556 Figure 5. Putative degradation pathway of BP3. Hypothesized degradation pathway
557 of BP3 based upon the online prediction tool “EAWAG-BBD Pathway Prediction
558 System” (<http://eawag-bbd.ethz.ch/predict/>)

559

560

561

562

563

564 **References:**

565 Armengaud, J., Happe, B., Timmis, K.N., 1998. Genetic analysis of dioxin dioxygenase
566 of *Sphingomonas* sp. Strain RW1: catabolic genes dispersed on the genome. J.
567 Bacteriol. 180, 3954–3966.

568 Badia-Fabregat, M., Rodríguez-Rodríguez, C.E., Gago-Ferrero, P., Olivares, A., Piña, B.,

569 Díaz-Cruz, M.S., Vicent, T., Barceló, D., Caminal, G., 2012. Degradation of UV

570 filters in sewage sludge and 4-MBC in liquid medium by the ligninolytic
571 fungus *Trametes versicolor*. *J. Environ. Manage.* 104, 114–120.
572 <https://doi.org/10.1016/j.jenvman.2012.03.039>

573 Barr, L., Alamer, M., Darbre, P.D., 2018. Measurement of concentrations of four
574 chemical ultraviolet filters in human breast tissue at serial locations across
575 the breast. *J. Appl. Toxicol. JAT* 38, 1112–1120.
576 <https://doi.org/10.1002/jat.3621>

577 Basta, T., Keck, A., Klein, J., Stolz, A., 2004. Detection and Characterization of
578 Conjugative Degradative Plasmids in Xenobiotic-Degrading *Sphingomonas*
579 Strains. *J. Bacteriol.* 186, 3862. [https://doi.org/10.1128/JB.186.12.3862-](https://doi.org/10.1128/JB.186.12.3862-3872.2004)
580 [3872.2004](https://doi.org/10.1128/JB.186.12.3862-3872.2004)

581 Bolyen, E., Rideout, J.R., Dillon, M.R., Bokulich, N.A., Abnet, C.C., Al-Ghalith, G.A.,
582 Alexander, H., Alm, E.J., Arumugam, M., Asnicar, F., Bai, Y., Bisanz, J.E.,
583 Bittinger, K., Brejnrod, A., Brislawn, C.J., Brown, C.T., Callahan, B.J., Caraballo-
584 Rodríguez, A.M., Chase, J., Cope, E.K., Da Silva, R., Diener, C., Dorrestein, P.C.,
585 Douglas, G.M., Durall, D.M., Duvallet, C., Edwardson, C.F., Ernst, M., Estaki, M.,
586 Fouquier, J., Gauglitz, J.M., Gibbons, S.M., Gibson, D.L., Gonzalez, A., Gorlick, K.,
587 Guo, J., Hillmann, B., Holmes, S., Holste, H., Huttenhower, C., Huttley, G.A.,
588 Janssen, S., Jarmusch, A.K., Jiang, L., Kaehler, B.D., Kang, K.B., Keefe, C.R., Keim,
589 P., Kelley, S.T., Knights, D., Koester, I., Kosciulek, T., Kreps, J., Langille, M.G.I.,
590 Lee, J., Ley, R., Liu, Y.-X., Lofffield, E., Lozupone, C., Maher, M., Marotz, C.,
591 Martin, B.D., McDonald, D., McIver, L.J., Melnik, A.V., Metcalf, J.L., Morgan, S.C.,
592 Morton, J.T., Naimey, A.T., Navas-Molina, J.A., Nothias, L.F., Orchanian, S.B.,

593 Pearson, T., Peoples, S.L., Petras, D., Preuss, M.L., Pruesse, E., Rasmussen, L.B.,
594 Rivers, A., Robeson, M.S., Rosenthal, P., Segata, N., Shaffer, M., Shiffer, A.,
595 Sinha, R., Song, S.J., Spear, J.R., Swafford, A.D., Thompson, L.R., Torres, P.J.,
596 Trinh, P., Tripathi, A., Turnbaugh, P.J., Ul-Hasan, S., van der Hooft, J.J.J., Vargas,
597 F., Vázquez-Baeza, Y., Vogtmann, E., von Hippel, M., Walters, W., Wan, Y.,
598 Wang, M., Warren, J., Weber, K.C., Williamson, C.H.D., Willis, A.D., Xu, Z.Z.,
599 Zaneveld, J.R., Zhang, Y., Zhu, Q., Knight, R., Caporaso, J.G., 2019. Reproducible,
600 interactive, scalable and extensible microbiome data science using QIIME 2.
601 Nat. Biotechnol. 37, 852–857. <https://doi.org/10.1038/s41587-019-0209-9>

602 Chen, Q., Wang, C.-H., Deng, S.-K., Wu, Y.-D., Li, Y., Yao, L., Jiang, J.-D., Yan, X., He, J., Li,
603 S.-P., 2014. Novel Three-Component Rieske Non-Heme Iron Oxygenase
604 System Catalyzing the N-Dealkylation of Chloroacetanilide Herbicides in
605 Sphingomonads DC-6 and DC-2. Appl. Environ. Microbiol. 80, 5078.
606 <https://doi.org/10.1128/AEM.00659-14>

607 Chen, Q., Yao, L., Wang, C., Deng, S., Chu, C., He, J., 2013. Isolation and
608 characterization of acetochlor-degrading strain Sphingomonas sp. DC-6 and
609 preliminary studies on its metabolic pathway. J. Agric. Sci. Technol. Beijing
610 15, 67–74.

611 Cheng, M., Yan, X., He, J., Qiu, J., Chen, Q., 2019. Comparative genome analysis reveals
612 the evolution of chloroacetanilide herbicide mineralization in Sphingomonas
613 wittichii DC-6. Arch. Microbiol. 201, 907–918.
614 <https://doi.org/10.1007/s00203-019-01660-w>

615 Coronado, E., Roggo, C., Johnson, D., van der Meer, J.R., 2012. Genome-Wide Analysis
616 of Salicylate and Dibenzofuran Metabolism in *Sphingomonas Wittichii* RW1.
617 *Front. Microbiol.* 3, 300. <https://doi.org/10.3389/fmicb.2012.00300>

618 Díaz-Cruz, M.S., Molins-Delgado, D., Serra-Roig, M.P., Kalogianni, E., Skoulikidis,
619 N.Th., Barceló, D., 2019. Personal care products reconnaissance in EVROTAS
620 river (Greece): Water-sediment partition and bioaccumulation in fish. *Sci.*
621 *Total Environ.* 651, 3079–3089.
622 <https://doi.org/10.1016/j.scitotenv.2018.10.008>

623 Fagervold, S.K., Rodrigues, A.S., Rohée, C., Roe, R., Bourrain, M., Stien, D., Lebaron, P.,
624 2019. Occurrence and Environmental Distribution of 5 UV Filters During the
625 Summer Season in Different Water Bodies. *Water. Air. Soil Pollut.* 230, 172.
626 <https://doi.org/10.1007/s11270-019-4217-7>

627 Fisher, M.M., Triplett, E.W., 1999. Automated approach for ribosomal intergenic
628 spacer analysis of microbial diversity and its application to freshwater
629 bacterial communities. *Appl Env. Microbiol* 65, 4630–4636.

630 Gago-Ferrero, P., Badia-Fabregat, M., Olivares, A., Piña, B., Blánquez, P., Vicent, T.,
631 Caminal, G., Díaz-Cruz, M.S., Barceló, D., 2012. Evaluation of fungal- and
632 photo-degradation as potential treatments for the removal of sunscreens BP3
633 and BP1. *Sci. Total Environ.* 427–428, 355–363.
634 <https://doi.org/10.1016/j.scitotenv.2012.03.089>

635 Gao, J., Ellis, L.B., Wackett, L.P., 2010. The University of Minnesota
636 Biocatalysis/Biodegradation Database: improving public access. *Nucleic*
637 *Acids Res* 38, D488.

638 Herlemann, D.P., Labrenz, M., Jürgens, K., Bertilsson, S., Waniek, J.J., Andersson, A.F.,
639 2011. Transitions in bacterial communities along the 2000 km salinity
640 gradient of the Baltic Sea. *ISME J.* 5, 1571–1579.
641 <https://doi.org/10.1038/ismej.2011.41>

642 Jin, C., Geng, Z., Pang, X., Zhang, Y., Wang, G., Ji, J., Li, X., Guan, C., 2019. Isolation and
643 characterization of a novel benzophenone-3-degrading bacterium
644 *Methylophilus* sp. strain FP-6. *Ecotoxicol. Environ. Saf.* 186, 109780.
645 <https://doi.org/10.1016/j.ecoenv.2019.109780>

646 Liu, Y.-S., Ying, G.-G., Shareef, A., Kookana, R.S., 2013. Degradation of Six Selected
647 Ultraviolet Filters in Aquifer Materials Under Various Redox Conditions.
648 *Groundw. Monit. Remediat.* 33, 79–88.
649 <https://doi.org/10.1111/gwmmr.12027>

650 Liu, Y.-S., Ying, G.-G., Shareef, A., Kookana, R.S., 2012. Biodegradation of the
651 ultraviolet filter benzophenone-3 under different redox conditions. *Environ.*
652 *Toxicol. Chem.* 31, 289–295. <https://doi.org/10.1002/etc.749>

653 Lozano C., Givens J., Stien D., Matallana-Surget S., Lebaron P., 2020. Bioaccumulation
654 and Toxicological Effects of UV-Filters on Marine Species, in: *The Handbook*
655 *of Environmental Chemistry*. Springer, Berlin, Heidelberg, pp. 1–46.

656 Mao, F., He, Y., Gin, K., 2018. Occurrence and fate of benzophenone-type UV filters in
657 aquatic environments: A review. *Environ. Sci. Water Res. Technol.* 5.
658 <https://doi.org/10.1039/C8EW00539G>

659 Marie, D., Partensky, F., Jacquet, S., Vaultot, D., 1997. Enumeration and Cell Cycle
660 Analysis of Natural Populations of Marine Picoplankton by Flow Cytometry
661 Using the Nucleic Acid Stain SYBR Green I. *Appl. Environ. Microbiol.* 63, 186.

662 Megharaj, M., Wittich, R.-M., Blasco, R., Pieper, D.H., Timmis, K.N., 1997. Superior
663 survival and degradation of dibenzo-p-dioxin and dibenzofuran in soil by
664 soil-adapted *Sphingomonas* sp. strain RW1. *Appl. Microbiol. Biotechnol.* 48,
665 109–114. <https://doi.org/10.1007/s002530051024>

666 Miller, T.R., Delcher, A.L., Salzberg, S.L., Saunders, E., Detter, J.C., Halden, R.U., 2010.
667 Genome sequence of the dioxin-mineralizing bacterium *Sphingomonas*
668 *wittichii* RW1. *J. Bacteriol.* 192, 6101–6102.
669 <https://doi.org/10.1128/JB.01030-10>

670 Molins-Delgado, D., Mánuez, M., Andreu, A., Hiraldo, F., Eljarrat, E., Barceló, D., Díaz-
671 Cruz, M.S., 2017. A Potential New Threat to Wild Life: Presence of UV Filters
672 in Bird Eggs from a Preserved Area. *Environ. Sci. Technol.* 51, 10983–10990.
673 <https://doi.org/10.1021/acs.est.7b03300>

674 Ramos, S., Homem, V., Alves, A., Santos, L., 2016. A review of organic UV-filters in
675 wastewater treatment plants. *Environ. Int.* 86, 24–44.
676 <https://doi.org/10.1016/j.envint.2015.10.004>

677 Rodríguez-Escales, P., Sanchez-Vila, X., 2020. Modeling the fate of UV filters in
678 subsurface: Co-metabolic degradation and the role of biomass in sorption
679 processes. *Water Res.* 168, 115192.
680 <https://doi.org/10.1016/j.watres.2019.115192>

681 Stien, D., Clergeaud, F., Rodrigues, A.M.S., Lebaron, K., Pillot, R., Romans, P.,
682 Fagervold, S., Lebaron, P., 2019. Metabolomics Reveal That Octocrylene
683 Accumulates in Pocillopora damicornis Tissues as Fatty Acid Conjugates and
684 Triggers Coral Cell Mitochondrial Dysfunction. Anal. Chem. 91, 990–995.
685 <https://doi.org/10.1021/acs.analchem.8b04187>

686 Suh, S., Pham, C., Smith, J., Mesinkovska, N.A., 2020. The banned sunscreen
687 ingredients and their impact on human health: a systematic review. Int. J.
688 Dermatol. <https://doi.org/10.1111/ijd.14824>

689 Wang, M., Carver, J.J., Phelan, V.V., Sanchez, L.M., Garg, N., Peng, Y., Nguyen, D.D.,
690 Watrous, J., Kapono, C.A., Luzzatto-Knaan, T., Porto, C., Bouslimani, A., Melnik,
691 A.V., Meehan, M.J., Liu, W.-T., Crüsemann, M., Boudreau, P.D., Esquenazi, E.,
692 Sandoval-Calderón, M., Kersten, R.D., Pace, L.A., Quinn, R.A., Duncan, K.R.,
693 Hsu, C.-C., Floros, D.J., Gavilan, R.G., Kleigrew, K., Northen, T., Dutton, R.J.,
694 Parrot, D., Carlson, E.E., Aigle, B., Michelsen, C.F., Jelsbak, L., Sohlenkamp, C.,
695 Pevzner, P., Edlund, A., McLean, J., Piel, J., Murphy, B.T., Gerwick, L., Liaw, C.-
696 C., Yang, Y.-L., Humpf, H.-U., Maansson, M., Keyzers, R.A., Sims, A.C., Johnson,
697 A.R., Sidebottom, A.M., Sedio, B.E., Klitgaard, A., Larson, C.B., Boya P, C.A.,
698 Torres-Mendoza, D., Gonzalez, D.J., Silva, D.B., Marques, L.M., Demarque, D.P.,
699 Pociute, E., O'Neill, E.C., Briand, E., Helfrich, E.J.N., Granatosky, E.A., Glukhov,
700 E., Ryffel, F., Houson, H., Mohimani, H., Kharbush, J.J., Zeng, Y., Vorholt, J.A.,
701 Kurita, K.L., Charusanti, P., McPhail, K.L., Nielsen, K.F., Vuong, L., Elfeki, M.,
702 Traxler, M.F., Engene, N., Koyama, N., Vining, O.B., Baric, R., Silva, R.R.,
703 Mascuch, S.J., Tomasi, S., Jenkins, S., Macherla, V., Hoffman, T., Agarwal, V.,

704 Williams, P.G., Dai, J., Neupane, R., Gurr, J., Rodríguez, A.M.C., Lamsa, A., Zhang,
705 C., Dorrestein, K., Duggan, B.M., Almaliti, J., Allard, P.-M., Phapale, P., Nothias,
706 L.-F., Alexandrov, T., Litaudon, M., Wolfender, J.-L., Kyle, J.E., Metz, T.O.,
707 Peryea, T., Nguyen, D.-T., VanLeer, D., Shinn, P., Jadhav, A., Müller, R., Waters,
708 K.M., Shi, W., Liu, X., Zhang, L., Knight, R., Jensen, P.R., Palsson, B.Ø., Pogliano,
709 K., Linington, R.G., Gutiérrez, M., Lopes, N.P., Gerwick, W.H., Moore, B.S.,
710 Dorrestein, P.C., Bandeira, N., 2016. Sharing and community curation of mass
711 spectrometry data with Global Natural Products Social Molecular
712 Networking. *Nat. Biotechnol.* 34, 828–837.
713 <https://doi.org/10.1038/nbt.3597>
714 Wittich, R.M., Wilkes, H., Sinnwell, V., Francke, W., Fortnagel, P., 1992. Metabolism of
715 dibenzo-p-dioxin by *Sphingomonas* sp. strain RW1. *Appl. Environ. Microbiol.*
716 58, 1005.
717
718
719